GEOLOGY | THE GEOLOGICAL SOCIETY OF AMERICA®

https://doi.org/10.1130/G52274.1

Manuscript received 7 April 2024
Revised manuscript received 6 September 2024
Manuscript accepted 20 September 2024

Published online 9 October 2024

Alkali-carbonate melts in the cratonic mantle evidenced by a wehrlite xenolith from the Majuagaa kimberlite, West Greenland

Ekaterina S. Kiseeva[1,2,*], Vadim S. Kamenetsky[3,4], Ivan F. Chayka[5], Roland Maas[6], and Troels F.D. Nielsen[7]

[1]American Museum of Natural History, New York, New York 10024, USA
[2]School of Biological, Earth & Environmental Sciences, University College Cork, Cork T23 TK30, Ireland
[3]Center of Deep Sea Research, Institute of Oceanology, Chinese Academy of Sciences, Qingdao 266003, China
[4]Institute of Volcanology and Seismology, 683006 Petropavlovsk-Kamchatsky, Russia
[5]D.S. Korzhinskii Institute of Experimental Mineralogy, 142432 Chernogolovka, Russia
[6]School of Geography, Earth and Atmospheric Sciences, University of Melbourne, Parkville, Victoria 3010, Australia
[7]Geological Survey of Denmark and Greenland, Øster Voldgade 10, DK-1350 Copenhagen K, Denmark

ABSTRACT

Carbonate melts are critically important for the deep carbon cycle, mantle melting, redox reactions, and transport of highly incompatible elements. The presence of carbonate melts in the cratonic mantle has been inferred from experimental studies, metasomatic transformations, and melt/fluid inclusions in xenoliths, kimberlites, and diamonds. However, the exact composition of such melts is difficult to determine due to their ephemeral nature and highly reactive properties. Once formed, they migrate away from the source and react with silicate mantle minerals, especially orthopyroxene, causing mantle metasomatism. Wehrlite is one of the products of interaction between the carbonate melt and peridotitic mantle and hence is an excellent candidate for locating in situ carbonate melts. Here, we report petrological, geochemical, and melt inclusion data for a garnet wehrlite xenolith in the Majuagaa kimberlite dike, West Greenland. The xenolith, which last equilibrated with the mantle at 4.5 GPa and 1000 °C, contains abundant melt pools composed of dolomite, calcite, serpentine, spinel, apatite, and phlogopite. Although the original magmatic mineralogy was largely destroyed by low-temperature alteration, remnants of the crystallized carbonatitic melt are preserved as primary melt inclusions in the liquidus Ti-Mg-Fe spinel. These melt inclusions, composed of carbonates, alkali carbonates, periclase/brucite, and minor halides, K-sulfide, apatite, and phlogopite, are the first direct evidence for in situ alkali-carbonate melt in the deep cratonic mantle. Compositionally, they are very similar to primary Na-dolomite melt found in experiments and in fluid inclusions within diamonds.

INTRODUCTION

Observations in mantle xenoliths and inclusions in diamonds as well as experimental studies indicate that carbonate melts are a significant component of Earth's carbon cycle and ubiquitous in Earth's cratonic mantle. Due to the ability to transport a large range of incompatible elements, low-degree carbonate melts are instrumental in causing cryptic and modal metasomatism of the lithosphere (Kamenetsky et al., 2004; Kiseeva et al., 2017). Their geochemical signature and imprint are found in mantle-derived magmas from diverse tectonic settings in all continents (Yaxley et al., 2019). Low-degree carbonate melts are highly reactive in their passage through the silicate lithosphere, and they are prone to complete exhaustion before they may reach the surface, making their exact compositions difficult to determine (Kamenetsky et al., 2004; Kamenetsky and Yaxley, 2015; Wallace and Green, 1988). Constraints on the chemical and physical properties of carbonate melts are largely based on experimental studies (e.g., Kiseeva et al., 2012) and geochemical (e.g., incompatible trace-element enrichment) and mineralogical (e.g., carbonate, halides, apatite, etc.) characteristics of xenoliths thought to be derived from metasomatized mantle (e.g., Yaxley et al., 1998).

Although mantle xenoliths and their inferred metasomatic alteration have been extensively studied, direct evidence for carbonate melts remains scarce. For example, alkali-rich carbonatitic melts have been found as secondary inclusions in olivine from deep-seated sheared peridotites (Golovin et al., 2018, 2020) and in ilmenite from mantle-derived polymict breccia (Giuliani et al., 2012).

The composition of mantle carbonate melts can be inferred from lithospheric wehrlite—an orthopyroxene-free, clinopyroxene-rich peridotite widely considered to be formed in equilibrium with carbonate melts (e.g., Aulbach et al., 2020; Yaxley and Green, 1996, and references therein).

Here we describe abundant, large-sized interstitial melt pools and associated well-preserved melt inclusions in a wehrlite xenolith from the diamond-bearing Majuagaa kimberlite in West Greenland. Our results provide the first evidence for the alkali-carbonate composition of such melt pools and veins and show that alkali-carbonate melts are circulating at large depths in the cratonic mantle.

METHODS

Major element concentrations reported in Table 1 were acquired using a JEOL JXA-8530F Plus electron microprobe using wavelength X-ray spectroscopy at the University of Tasmania. Melt inclusions in spinel (Fig. 2; Figs. S5 and S6 in the Supplemental Material[1])

Ekaterina S. Kiseeva https://orcid.org/0000-0002-5781-5716
*kkiseeva@amnh.org

[1]Supplemental Material. Description of the Rb-Sr and Sm-Nd isotopic analyses and results, Table S1, Figures S1–S6, and additional references. Please visit https://doi.org/10.1130/GEOL.S.27089605 to access the supplemental material; contact editing@geosociety.org with any questions.

CITATION: Kiseeva, E.S., et al., 2024, Alkali-carbonate melts in the cratonic mantle evidenced by a wehrlite xenolith from the Majuagaa kimberlite, West Greenland: Geology, v. XX, p. , https://doi.org/10.1130/G52274.1

TABLE 1. AVERAGE COMPOSITIONS (IN wt%) OF MAIN MINERALS OF (i) WEHRLITE XENOLITH GGU477406 AND (ii) OF MELT INCLUSIONS HOSTED BY SPINEL IN "MELT POOLS" IN THIS XENOLITH

	Olivine	σ	Garnet	σ	Clinopyroxene	σ	Spinel core	σ	Spinel rim	σ	Melt
n	10		10		10		22		9		5
SiO_2	41.44	0.12	40.00	0.20	54.97	0.19	n.m.	—	n.m.	—	b.d.l.
TiO_2	n.m.	—	0.88	0.02	0.21	0.01	13.40	1.02	1.08	0.43	1.64
Al_2O_3	b.d.l.	—	13.51	0.11	1.41	0.05	7.77	1.10	1.17	0.47	b.d.l.
Cr_2O_3	0.05	0.01	11.92	0.05	2.58	0.05	0.63	0.50	0.08	0.06	b.d.l.
FeO_t	7.18	0.09	6.61	0.04	2.08	0.01	51.19	2.05	76.11	0.98	5.76
NiO	0.38	0.01	n.m.	—	n.m.	—	0.18	0.04	0.13	0.03	b.d.l.
MnO	0.11	0.01	0.41	0.01	0.09	0.01	0.45	0.05	0.44	0.13	b.d.l.
MgO	51.35	0.06	16.68	0.10	16.93	0.08	21.10	0.49	12.82	1.04	19.37
CaO	b.d.l.	—	9.88	0.03	20.23	0.03	n.m.	—	n.m.	—	23.42
Na_2O	n.m.	—	0.06	0.02	1.68	0.06	n.m.	—	n.m.	—	3.94
K_2O	b.d.l.	—	b.d.l.	—	b.d.l.	—	b.d.l.	—	b.d.l.	—	4.94
ZrO_2	n.m.	—	n.m.	—	n.m.	—	0.26	0.13	0.23	0.11	n.m.
V_2O_3	n.m.	—	n.m.	—	n.m.	—	0.27	0.03	0.50	0.08	n.m.
TOTAL	100.55	0.21	99.96	0.32	100.17	0.22	95.26	0.37	92.55	0.45	59.07*
Mg#	0.93		0.82		0.94		0.76		0.65		

Note: FeOt—total FeO; where average FeO and Fe_2O_3 in spinel cores and rims, calculated on the basis of spinel stoichiometry, are 11.80 wt% and 43.77 wt% and 12.03 wt% and 71.20 wt%, respectively. Mg#—Mg/(Mg + Fe^{2+}); b.d.l.—below detection limit; n.m.—not measured.
*Excluding CO_2, Cl, S, P, Ba, etc.

were analyzed on a Hitachi SU-70 field emission scanning electron microscope equipped with an Oxford AZtec Energy XMax 80 detector using energy-dispersive X-ray spectroscopy (University of Tasmania). The same instrument was used for back-scattered electron images presented in Figures 1 and S3–S4. Rb-Sr and Sm-Nd isotopic analyses of the xenolith and host kimberlite were carried out by isotope dilution multi-collector inductively coupled plasma–mass spectrometry at the University of Melbourne.

MELT POOLS IN WEHRLITE

The Majuagaa kimberlite dike (ca. 560 Ma; Tappe et al., 2011), located in Archean rocks of the Maniitsoq region, southern West Greenland (Fig. S1), is a weakly altered, diamondiferous kimberlite (Nielsen et al., 2009). The xenolith suite within this kimberlite includes the undeformed, coarse-grained peridotite xenolith GGU477406, which lacks orthopyroxene, has specific mineral compositions, and thus is classified as a garnet wehrlite (Fig. 1A; Fig. S2). Major-element compositions of olivine, clinopyroxene, and garnet from the wehrlite are presented in Table 1. Olivine has Mg# = 93, and clinopyroxene is diopsidic with subordinate amounts of enstatite and CaCr-Tschermak components. Garnet is rich in Mg and Cr and shows "wehrlite" CaO-Cr_2O_3 relationships (Fig. S2; Sobolev et al., 1973).

Interstitial to the wehrlite minerals, abundant "pinch-and-swell"–textured material, sometimes showing ocelli-like teardrop features (Fig. 1), is reminiscent of crystallized melt pools (Fig. S3). These features are mainly composed of carbonate masses (predominantly dolomite and subordinate calcite), serpentine rimmed by Fe oxides in ocelli, Na- and Sr-rich apatite, spinel, and phlogopite/tetraferriphlogopite, along with minor Fe-Ni sulfides, djerfisherite, sylvite, barite, and halite (Figs. 1A and 1B; Fig. S3). The carbonate masses contain micrometer-sized multiphase inclusions composed of Na-Ca, K-Ca, and Na-K-Ca carbonates, Sr-Ba carbonates (i.e., burbankite), Sr-La-Ce sulfates, Na-K chlorides (halite, sylvite), barite, apatite, and fluorite (Fig. 2B; Fig. S4), a phase assemblage known from experimental and natural carbonatites (Anenburg et al., 2020; Mororó et al., 2024). Apart from rare phlogopite, silicates appear to be absent.

Among the minerals in the carbonate-rich melt pools, spinel is of particular interest (Figs. 2C–2G; Figs. S5–S6; Table 1). Occurring as solitary or intergrown euhedral crystals showing well-developed zoning, the spinels are noteworthy for Cr-free, Zr-rich compositions (up to 0.62 wt% ZrO_2; average = 0.24 wt% ZrO_2). Spinel cores high in TiO_2, FeO_{tot}, and MgO are surrounded by a zone rich in FeO_{tot} and MgO and poor in TiO_2 and Al_2O_3. Some crystals have a thin magnetite rim (Figs. 2C–2G; Figs. S5–S6). The spinel cores contain single- to multiphase inclusions (<1–20 μm in diameter; Figs. 2C–2G; Figs. S5–S6), which have been difficult to characterize due to their host's opacity. Inclusions in approximately 50 polished spinel grains are variably composed of dolomite, Na-dolomite, alkali-rich carbonate (nyerereite), periclase, apatite, K-Fe-Ni sulfide (djerfisherite), sylvite, and F-bearing (up to 4 wt%) brucite (Figs. 2C–2G; Figs. S5–S6), and we suggest they represent daughter minerals in primary melt inclusions. Although the large number of grains examined suggests this list of minerals is representative, other alkali-bearing carbonates may be present, but their identification by energy-dispersive X-ray spectroscopy (EDS) is hampered by small size, rapid degradation under the electron beam, and hydration reactions on contact with atmospheric moisture.

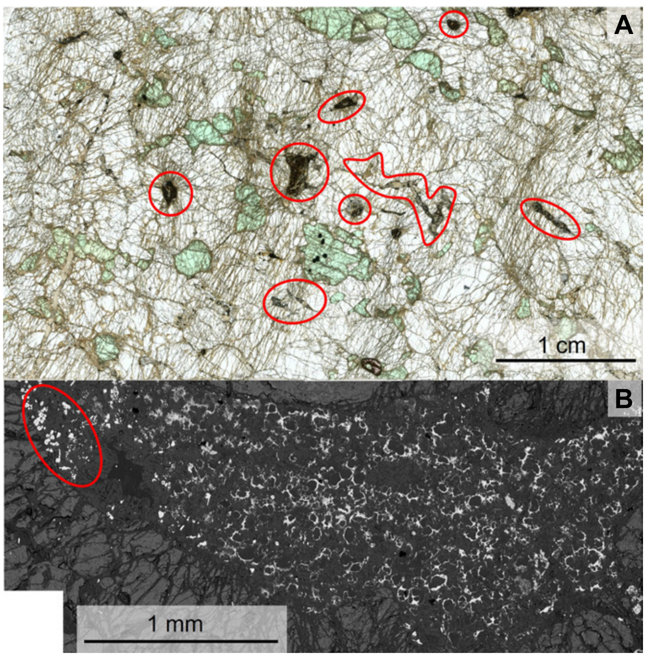

Figure 1. (A) Plain transparent light image of thin section of garnet wehrlite xenolith GGU477406, showing fractured olivine (colorless), clinopyroxene (green), and melt pools (highlighted in red). (B) Backscattered electron (BSE) image of "pinch-and-swell"–textured domains in xenolith, which are composed of dolomite and serpentine and rimmed by magnetite. Other minor constituents are calcite, apatite, phlogopite, sulfides, and accumulations of Ti-Mg-Fe spinel (red oval).

ALKALI-CARBONATE MELTS IN THE MANTLE

The Archean crust of southern West Greenland contains numerous Neoproterozoic (ca. 550–600 Ma) alkaline magmatic complexes,

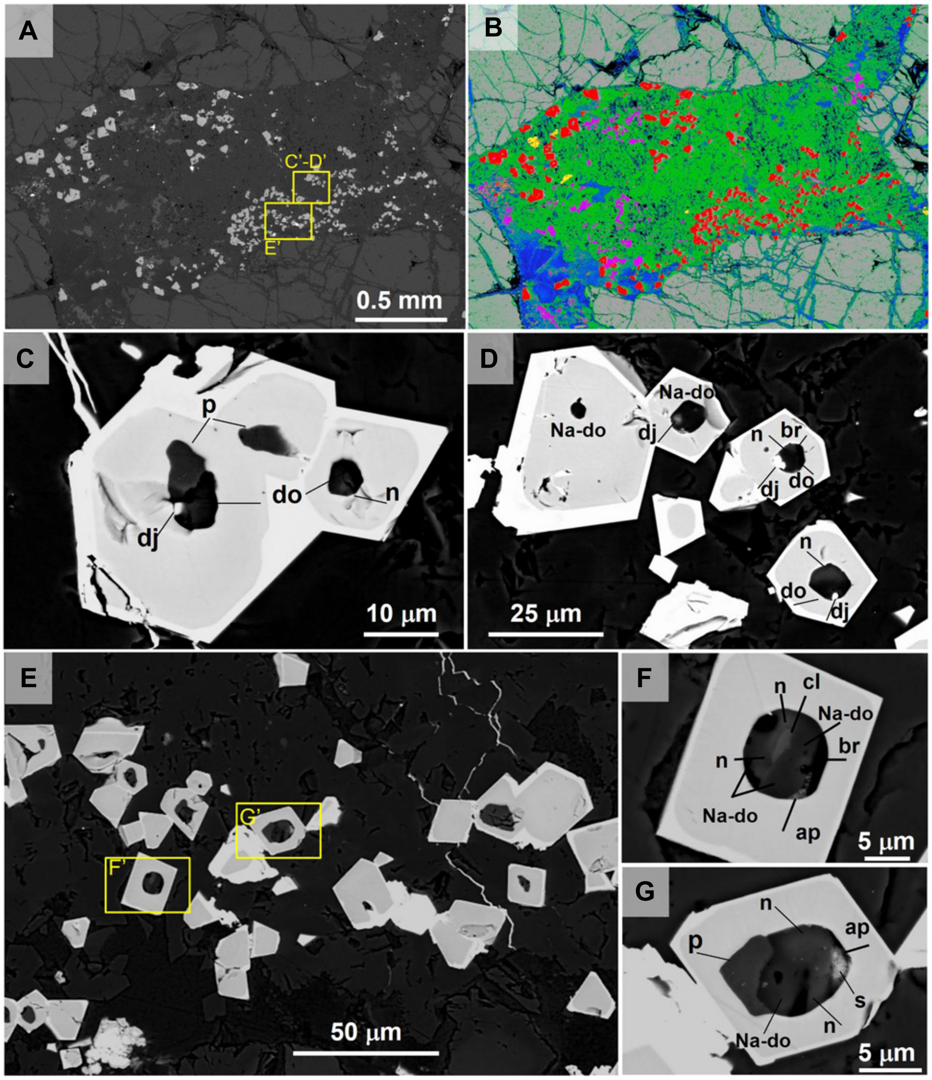

Figure 2. (A, B) Backscattered electron (BSE) and false color images, respectively, showing abundant zoned spinel crystals (red) in carbonate melt pool composed of dolomite (green), serpentine (blue), calcite (cyan), and minor apatite and phlogopite (both yellow) in wehrlite xenolith GGU477406. (C–E) Close-up BSE images of boxed areas shown in A. (F–G) Close-up BSE images of boxed areas in image E, showing crystallized melt inclusions. Daughter minerals in melt inclusions are dominated by dolomite (do), Na-dolomite (Na-do), periclase (p), calcite (cl), and nyerereite (n) with minor apatite (ap), sylvite (s), djerfisherite (dj), and F-bearing (4 wt%) brucite (br).

including ultramafic lamprophyres, aillikites, carbonatites, and kimberlites (Kamenetsky et al., 2009; Nielsen et al., 2009; Tappe et al., 2009). The Majuagaa carbonate-rich kimberlite appears to be similar to other kimberlites in the Maniitsoq region in terms of textures, compositions, and megacryst-macrocryst-xenolith suites (Nielsen and Sand, 2008), suggesting it represents the regional subcontinental lithospheric mantle (SCLM). This is supported by Sr-Nd isotopic data ($^{87}Sr/^{86}Sr = 0.7025–0.7042$, $\varepsilon_{Nd} = \sim+3$) from the kimberlite and the wehrlite xenolith reported here (see Supplemental Material).

Geochemical modeling of the Majuagaa kimberlite suggests its parental melt was derived from a Mg-rich silicocarbonatitic melt that formed at near-solidus temperatures in the SCLM (Nielsen and Sand, 2008; Pilbeam et al., 2023; Tappe et al., 2011). Xenolith GGU477406 is considered to be a sample of the SCLM that experienced both carbonatization and low-degree partial melting. Based on clinopyroxene thermobarometry, the wehrlite resided at 4.5 GPa and 1000 °C prior to entrainment in the kimberlitic magma (Nimis and Taylor, 2000; Sudholz et al., 2021). These pressure-temperature conditions are consistent with a 40 mW/m^2 geotherm as constrained using garnet lherzolite xenoliths from nearby localities in West Greenland (Sand et al., 2009).

The abundant melt pools and veinlets in this xenolith are thought to reflect processes related to the wehrlitization of preexisting mantle peridotite (Dalton and Wood, 1993; Yaxley et al., 1991), where reaction between carbonate or alkali-carbonate melt and mantle lherzolite (Aulbach et al., 2020) at ≥4.5 GPa would have resulted in removal of orthopyroxene and crystallization of clinopyroxene and CaCr-rich garnet (Table 1; Fig. S2) to produce the wehrlite lithology. In the case of xenolith GGU477406, it is likely that the excess of the carbonate melt remained in the system after the wehrlitization process was complete. Moreover, the observed globular textures in the inferred melt pools (Fig. 1B; Fig. S3) may reflect immiscibility between the parental carbonate melt and a silicate component. According to experimental studies, carbonate melt in equilibrium with peridotite at mantle pressures contains ~3–5 wt% SiO_2 (Sweeney, 1994), and this silicate component would unmix from the parental carbonate melt as the immiscibility field expanded with decreasing temperature (Berkesi et al., 2023; Brooker and Kjarsgaard, 2011; Kamenetsky and Yaxley, 2015) and pressure (Antonelli et al., 2023).

Unfortunately, inferring melt compositions from the xenolith's melt pool mineralogy is complicated by alteration. We observed abundant carbonates and other phases (apatite, spinel-group minerals, sulfates, chlorides, phlogopite/tetraferriphlogopite, djerfisherite, etc.) in a calcite-dolomite matrix surrounded by spherical and kidney-shaped droplets composed of serpentine and rimmed by Fe oxide (Fig. 1B; Fig. S3). Based on comparison with other potential examples of liquid immiscibility in mantle xenoliths (Pyle and Haggerty, 1994; Soltys et al., 2016) and our observation that the magnetite-rimmed ocelli in the studied xenolith melt pools are mainly composed of silicates (serpentine/talc/chlorite) while the matrix has a carbonate composition (dolomitic), the former coexistence of carbonate and silicate melts appears to be likely. This is supported by experimental study on orthopyroxene–Na_2CO_3 starting material performed at 2–5 GPa and 1000–1200 °C, which produced ocelli-like teardrop-shaped textures much like those observed in the wehrlite melt pools (Kamenetsky and Yaxley, 2015).

The compositions of fluids and melts within the SCLM are difficult to constrain, in part because the minerals used to identify such compositions, such as calcite and dolomite, cannot be assumed to preserve primary compositions. In contrast, small samples of carbonate melt present at different stages of their host mantle's evolution are remarkably well preserved within inclusions in magmatic spinel (Figs. 2C–2G). The liquidus nature of spinel crystals in melt pool assemblages within GGU477406 can be inferred from their composition and zoning patterns, which are reminiscent of spinels in calcitic kimberlites worldwide (e.g., Mitchell, 1995). Importantly, the spinels are very low in Cr_2O_3

(0.63 wt%) and rich in Fe, Mg, and Ti, reinforcing the interpretation of crystallization from a carbonate melt.

Minerals included within the spinel, although indicative of a closed system, are unlikely to be in equilibrium with each other because of the gradual pressure-temperature changes that occurred during the xenolith's ascent to the surface. By contrast, the association of melt inclusions with liquidus spinel, their alignment within crystallographically controlled growth zones in their spinel hosts (Fig. S4), and the absence of melt-filled cracks are all strong indicators of a primary origin; i.e., the melt inclusions are representative of the melt from which the spinel crystallized. Moreover, there is a striking difference between those intact inclusions, usually $<20\ \mu m$, which represent crystalline products of the residual melt, and the inclusions intersected by fractures, which contain dolomite and/or serpentine only.

X-ray element mapping of the larger melt inclusions recorded average major-element concentrations of 23 ± 3 wt% CaO, 19 ± 4 wt% MgO, 6 ± 3 wt% FeO, 5 ± 3 wt% K_2O, 4 ± 2 wt% Na_2O, and 2 ± 1 wt% TiO_2 (Table 1), which are remarkably similar to the compositions of carbonate liquids produced in experiments (e.g., Sweeney, 1994; Thibault et al., 1992; Wallace and Green, 1988), and to high-Mg carbonate compositions found in fluid inclusions in diamonds (Weiss et al., 2011). This indicates the melt inclusions preserve the composition of alkali carbonate melts generated within the mantle source of the kimberlite.

Despite the alteration issues mentioned earlier, alkali-rich carbonatitic initial melt signatures can also be inferred from phase assemblages in the large melt pools present in the wehrlite (Figs. 1B, 2A, and 2B; Fig. S3). The inclusions of sulfides and K-Na chlorides in the dolomite matrix indicate sulfur- and chlorine-rich carbonate liquids, while Na-rich apatite and K-bearing minerals (phlogopite/tetraferriphlogopite, djerfisherite) further confirm the alkali-rich composition of the parental carbonate melt. Although the melt represented by the melt pools is likely to have formed at lower pressures and represents carbonate melt that has lost its original silicate component, it provides strong additional evidence in support of the presence of alkali-carbonate melts in the lithospheric mantle.

Additional support for genetic links among carbonate melt metasomatism, kimberlite formation, and wehrlitization is provided by the Rb-Sr and Sm-Nd isotope results acquired during this study (see Supplemental Material). Step-leaching of the kimberlite yielded water- and HCl-soluble fractions, which combine with the silicate/oxide-rich residue to produce a Rb-Sr isochron age (551 ± 68 Ma) close to the ca. 560 Ma emplacement age of the Majuagaa complex. The carbonate ($^{87}Sr/^{86}Sr = 0.7042$, $\varepsilon_{Nd} = +3$) is isotopically similar to the kimberlite. Likewise, a carbonate fraction produced by reaction with HCl within the wehrlite xenolith defined a ca. 595 Ma Sm-Nd age with associated clinopyroxene, recording wehrlite formation during the Neoproterozoic kimberlite event. The isotopic signatures of these phases (clinopyroxene $^{87}Sr/^{86}Sr = 0.7025$, $\varepsilon_{Nd} = +3.5$; carbonate $^{87}Sr/^{86}Sr = 0.7034$, $\varepsilon_{Nd} = +3.2$) are consistent with the host kimberlite composition defined here and in Tappe et al. (2011).

CONCLUDING REMARKS

Carbonate melts are powerful metasomatic agents, and their geochemical signatures and imprints are found in mantle-derived magmatic rocks from diverse tectonic settings in all continents. The results of this study represent the first known example of in situ primary alkali-rich carbonate melts preserved as inclusions in spinel phenocrysts from carbonate-rich melt pools in a mantle wehrlite. Our findings also provide evidence for the genetic link between carbonate metasomatism and the formation of wehrlite, an orthopyroxene-free mantle peridotite.

ACKNOWLEDGMENTS

Maya Kamenetsky and Karsten Gömann helped with sample preparation and analytical work at the University of Tasmania. We thank Rondi Davies for valuable discussions. We thank Marc Norman for editorial handling. Sebastian Tappe and two anonymous reviewers provided insightful comments that helped to improve the manuscript. We acknowledge support from Natural Environment Research Council (NERC) grant NE/L010828/1 and Irish Research Council grant IRCLA/2022/2638 to E.S. Kiseeva and funding from the Chinese Academy of Sciences to V.S. Kamenetsky. I.F. Chayka was supported by FMUF-2022-0004 research programme of the Russian Academy of Sciences.

REFERENCES CITED

Anenburg, M., Mavrogenes, J.A., Frigo, C., and Wall, F., 2020, Rare earth element mobility in and around carbonatites controlled by sodium, potassium, and silica: Science Advances, v. 6, no. 41, https://doi.org/10.1126/sciadv.abb6570.

Antonelli, M.A., Sartori, G., Giuliani, A., Schauble, E.A., Hoffmann, J., and Schmidt, M.W., 2023, Calcium isotope fractionation during melt immiscibility and carbonatite petrogenesis: Geochemical Perspectives Letters, v. 28, p. 13–19, https://doi.org/10.7185/geochemlet.2338.

Aulbach, S., Lin, A.B., Weiss, Y., and Yaxley, G.M., 2020, Wehrlites from continental mantle monitor the passage and degassing of carbonated melts: Geochemical Perspectives Letters, v. 15, p. 30–34, https://doi.org/10.7185/geochemlet.2031.

Berkesi, M., Myovela, J.L., Yaxley, G.M., and Guzmics, T., 2023, Carbonatite formation in continental settings via high pressure–high temperature liquid immiscibility: Geochimica et Cosmochimica Acta, v. 349, p. 41–54, https://doi.org/10.1016/j.gca.2023.03.027.

Brooker, R.A., and Kjarsgaard, B.A., 2011, Silicate-carbonate liquid immiscibility and phase relations in the system SiO_2-Na_2O-Al_2O_3-CaO-CO_2 at 0.1–2.5 GPa with applications to carbonatite genesis: Journal of Petrology, v. 52, no. 7–8, p. 1281–1305, https://doi.org/10.1093/petrology/egq081.

Dalton, J.A., and Wood, B.J., 1993, The compositions of primary carbonate melts and their evolution through wallrock reaction in the mantle: Earth and Planetary Science Letters, v. 119, no. 4, p. 511–525, https://doi.org/10.1016/0012-821X(93)90059-I.

Giuliani, A., Kamenetsky, V.S., Phillips, D., Kendrick, M.A., Wyatt, B.A., and Goemann, K., 2012, Nature of alkali-carbonate fluids in the sub-continental lithospheric mantle: Geology, v. 40, no. 11, p. 967–970, https://doi.org/10.1130/G33221.1.

Golovin, A.V., Sharygin, I.S., Kamenetsky, V.S., Korsakov, A.V., and Yaxley, G.M., 2018, Alkali-carbonate melts from the base of cratonic lithospheric mantle: Links to kimberlites: Chemical Geology, v. 483, p. 261–274, https://doi.org/10.1016/j.chemgeo.2018.02.016.

Golovin, A.V., Sharygin, I.S., Korsakov, A.V., Kamenetsky, V.S., and Abersteiner, A., 2020, Can primitive kimberlite melts be alkali-carbonate liquids: Composition of the melt snapshots preserved in deepest mantle xenoliths: Journal of Raman Spectroscopy, v. 51, no. 9, p. 1849–1867, https://doi.org/10.1002/jrs.5701.

Kamenetsky, M.B., Sobolev, A.V., Kamenetsky, V.S., Maas, R., Danyushevsky, L.V., Thomas, R., Pokhilenko, N.P., and Sobolev, N.V., 2004, Kimberlite melts rich in alkali chlorides and carbonates: A potent metasomatic agent in the mantle: Geology, v. 32, no. 10, p. 845–848, https://doi.org/10.1130/G20821.1.

Kamenetsky, V.S., and Yaxley, G.M., 2015, Carbonate-silicate liquid immiscibility in the mantle propels kimberlite magma ascent: Geochimica et Cosmochimica Acta, v. 158, p. 48–56, https://doi.org/10.1016/j.gca.2015.03.004.

Kamenetsky, V.S., Kamenetsky, M.B., Weiss, Y., Navon, O., Nielsen, T.F.D., and Mernagh, T.P., 2009, How unique is the Udachnaya-East kimberlite? Comparison with kimberlites from the Slave craton (Canada) and SW Greenland: Lithos, v. 112, p. 334–346, https://doi.org/10.1016/j.lithos.2009.03.032.

Kiseeva, E.S., Yaxley, G.M., Hermann, J., Litasov, K.D., Rosenthal, A., and Kamenetsky, V.S., 2012, An experimental study of carbonated eclogite at 3.5–5.5 GPa—Implications for silicate and carbonate metasomatism in the cratonic mantle: Journal of Petrology, v. 53, no. 4, p. 727–759, https://doi.org/10.1093/petrology/egr078.

Kiseeva, E.S., Kamenetsky, V.S., Yaxley, G.M., and Shee, S.R., 2017, Mantle melting versus mantle metasomatism—"The chicken or the egg" dilemma: Chemical Geology, v. 455, p. 120–130, https://doi.org/10.1016/j.chemgeo.2016.10.026.

Mitchell, R.H., 1995, Kimberlites, Orangeites, and Related Rocks: New York, Plenum Press, 410 p.

Mororó, E.A.A., Berkesi, M., Zajacz, Z., and Guzmics, T., 2024, Rare earth element transport and mineralization linked to fluids from carbonatite systems: Geology, v. 52, no. 4, p. 240–244, https://doi.org/10.1130/G51531.1.

Nielsen, T.F.D., and Sand, K.K., 2008, The Majuagaa kimberlite dike, Maniitsoq region, West Greenland: Constraints on an Mg-rich silicocarbonatitic melt composition from groundmass mineralogy and bulk compositions: Canadian Mineralogist, v. 46, p. 1043–1061, https://doi.org/10.3749/canmin.46.4.1043.

Nielsen, T.F.D., Jensen, S.M., Secher, K., and Sand, K.K., 2009, Distribution of kimberlite and aillikite in the Diamond Province of southern West Greenland: A regional perspective based on groundmass mineral chemistry and bulk compositions: Lithos, v. 112, p. 358–371, https://doi.org/10.1016/j.lithos.2009.05.035.

Nimis, P., and Taylor, W.R., 2000, Single clinopyroxene thermobarometry for garnet peridotites. Part I. Calibration and testing of a Cr-in-Cpx barometer and an enstatite-in-Cpx thermometer: Contributions to Mineralogy and Petrology, v. 139, no. 5, p. 541–554, https://doi.org/10.1007/s004100000156.

Pilbeam, L., Rasmussen, T.M., Waight, T., and Nielsen, T., 2023, Inverse modeling to constrain composition of CO_2-rich parental melt of kimberlite: Model development and application to the Majuagaa dyke, southern West Greenland: Journal of Petrology, v. 64, no. 2, https://doi.org/10.1093/petrology/egac127.

Pyle, J.M., and Haggerty, S.E., 1994, Silicate-carbonate liquid immiscibility in upper-mantle eclogites—Implications for natrosilicic and carbonatitic conjugate melts: Geochimica et Cosmochimica Acta, v. 58, no. 14, p. 2997–3011, https://doi.org/10.1016/0016-7037(94)90174-0.

Sand, K.K., Waight, T.E., Pearson, D.G., Nielsen, T.F.D., Makovicky, E., and Hutchison, M.T., 2009, The lithospheric mantle below southern West Greenland: A geothermobarometric approach to diamond potential and mantle stratigraphy: Lithos, v. 112, p. 1155–1166, https://doi.org/10.1016/j.lithos.2009.05.012.

Sobolev, N.V., Lavrent'ev, Y.G., Pokhilenko, N.P., and Usova, L.V., 1973, Chrome-rich garnets from kimberlites of Yakutia and their parageneses: Contributions to Mineralogy and Petrology, v. 40, no. 1, p. 39–52, https://doi.org/10.1007/BF00371762.

Soltys, A., Giuliani, A., Phillips, D., Kamenetsky, V.S., Maas, R., Woodhead, J., and Rodemann, T., 2016, In-situ assimilation of mantle minerals by kimberlitic magmas—Direct evidence from a garnet wehrlite xenolith entrained in the Bultfontein kimberlite (Kimberley, South Africa): Lithos, v. 256–257, p. 182–196, https://doi.org/10.1016/j.lithos.2016.04.011.

Sudholz, Z.J., Yaxley, G.M., Jaques, A.L., and Brey, G.P., 2021, Experimental recalibration of the Cr-in-clinopyroxene geobarometer: Improved precision and reliability above 4.5 GPa: Contributions to Mineralogy and Petrology, v. 176, 11, https://doi.org/10.1007/s00410-020-01768-z.

Sweeney, R.J., 1994, Carbonatite melt compositions in the Earth's mantle: Earth and Planetary Science Letters, v. 128, no. 3–4, p. 259–270, https://doi.org/10.1016/0012-821X(94)90149-X.

Tappe, S., Steenfelt, A., Heaman, L.M., and Simonetti, A., 2009, The newly discovered Jurassic Tikiusaaq carbonatite-aillikite occurrence, West Greenland, and some remarks on carbonatite-kimberlite relationships: Lithos, v. 112, p. 385–399, https://doi.org/10.1016/j.lithos.2009.03.002.

Tappe, S., Pearson, D.G., Nowell, G., Nielsen, T., Milstead, P., and Muehlenbachs, K., 2011, A fresh isotopic look at Greenland kimberlites: Cratonic mantle lithosphere imprint on deep source signal: Earth and Planetary Science Letters, v. 305, no. 1–2, p. 235–248, https://doi.org/10.1016/j.epsl.2011.03.005.

Thibault, Y., Edgar, A.D., and Lloyd, F.E., 1992, Experimental investigation of melts from a carbonated phlogopite lherzolite—Implications for metasomatism in the continental lithospheric mantle: The American Mineralogist, v. 77, no. 7–8, p. 784–794.

Wallace, M.E., and Green, D.H., 1988, An experimental determination of primary carbonatite magma composition: Nature, v. 335, no. 6188, p. 343–346, https://doi.org/10.1038/335343a0.

Weiss, Y., Griffin, W.L., Bell, D.R., and Navon, O., 2011, High-Mg carbonatitic melts in diamonds, kimberlites and the sub-continental lithosphere: Earth and Planetary Science Letters, v. 309, no. 3–4, p. 337–347, https://doi.org/10.1016/j.epsl.2011.07.012.

Yaxley, G.M., and Green, D.H., 1996, Experimental reconstruction of sodic dolomitic carbonatite melts from metasomatised lithosphere: Contributions to Mineralogy and Petrology, v. 124, no. 3–4, p. 359–369, https://doi.org/10.1007/s004100050196.

Yaxley, G.M., Crawford, A.J., and Green, D.H., 1991, Evidence for carbonatite metasomatism in spinel peridotite xenoliths from western Victoria, Australia: Earth and Planetary Science Letters, v. 107, no. 2, p. 305–317, https://doi.org/10.1016/0012-821X(91)90078-V.

Yaxley, G.M., Green, D.H., and Kamenetsky, V., 1998, Carbonatite metasomatism in the southeastern Australian lithosphere: Journal of Petrology, v. 39, no. 11–12, p. 1917–1930, https://doi.org/10.1093/petroj/39.11-12.1917.

Yaxley, G.M., Ghosh, S., Kiseeva, E.S., Mallik, A., Spandler, C., Thomson, A.R., and Walter, M.J., 2019, CO_2-rich melts in Earth, *in* Orcutt, B.N., Daniel, I., and Dasgupta, R., eds., Deep Carbon: Past to Present: Cambridge, UK, Cambridge University Press, p. 129–162, https://doi.org/10.1017/9781108677950.006.

Printed in the USA